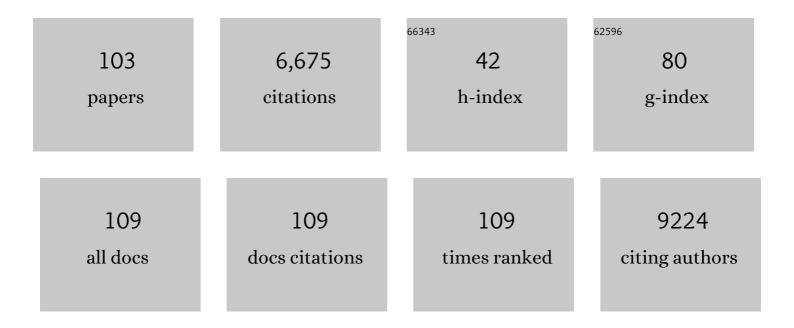
List of Publications by Year in descending order

Source: https://exaly.com/author-pdf/3531816/publications.pdf Version: 2024-02-01



HAO ZHANC

#	Article	IF	CITATIONS
1	Fe(III)â€ <b>6</b> hikonin Supramolecular Nanomedicine for Combined Therapy of Tumor via Ferroptosis and Necroptosis. Advanced Healthcare Materials, 2022, 11, e2101926.	7.6	25
2	Z-Scheme heterostructures for glucose oxidase-sensitized radiocatalysis and starvation therapy of tumors. Nanoscale, 2022, 14, 2186-2198.	5.6	8
3	Fe(III)-Doped Polyaminopyrrole Nanoparticle for Imaging-Guided Photothermal Therapy of Bladder Cancer. ACS Biomaterials Science and Engineering, 2022, 8, 502-511.	5.2	10
4	Metal Nanoclusters/Polyvinyl Alcohol Composite Films as the Alternatives for Fabricating Remote-Type White Light-Emitting Diodes. Nanomaterials, 2022, 12, 204.	4.1	5
5	Copper Ion and Ruthenium Complex Codoped Polydopamine Nanoparticles for Magnetic Resonance/Photoacoustic Tomography Imaging-Guided Photodynamic/Photothermal Dual-Mode Therapy. ACS Applied Bio Materials, 2022, 5, 2365-2376.	4.6	9
6	Surface Stabilization of Colloidal Perovskite Nanocrystals via Multi-amine Chelating Ligands. ACS Energy Letters, 2022, 7, 1963-1970.	17.4	34
7	Long-lasting photoluminescence quantum yield of cesium lead halide perovskite-type quantum dots. Frontiers of Chemical Science and Engineering, 2021, 15, 187-197.	4.4	2
8	Achieving full-color emission of Cu nanocluster self-assembly nanosheets by the virtue of halogen effects. Soft Matter, 2021, 17, 4550-4558.	2.7	5
9	Microwave-assisted synthesis of blue-emitting cesium bismuth bromine perovskite nanocrystals without polar solvent. Journal of Alloys and Compounds, 2021, 886, 161248.	5.5	6
10	Interstitial Nature of Mn <sup>2+</sup> Doping in 2D Perovskites. ACS Nano, 2021, 15, 20550-20561.	14.6	19
11	Targeted multifunctional nanomaterials with MRI, chemotherapy and photothermal therapy for the diagnosis and treatment of bladder cancer. Biomaterials Science, 2020, 8, 342-352.	5.4	33
12	BiVO <sub>4</sub> @Bi <sub>2</sub> S <sub>3</sub> Heterojunction Nanorods with Enhanced Charge Separation Efficiency for Multimodal Imaging and Synergy Therapy of Tumor. ACS Applied Bio Materials, 2020, 3, 5080-5092.	4.6	16
13	Self-Assembly of Au Nanoclusters into Helical Ribbons by Manipulating the Flexibility of Capping Ligands. Langmuir, 2020, 36, 14614-14622.	3.5	6
14	Enhanced charge separation and photocatalytic hydrogen evolution in carbonized-polymer-dot-coupled lead halide perovskites. Materials Horizons, 2020, 7, 2719-2725.	12.2	38
15	Efficacy of Fe <sub>3</sub> O <sub>4</sub> @polydopamine nanoparticle-labeled human umbilical cord Wharton's jelly-derived mesenchymal stem cells in the treatment of streptozotocin-induced diabetes in rats. Biomaterials Science, 2020, 8, 5362-5375.	5.4	10
16	Effect of Oleamine on Microwave-Assisted Synthesis of Cesium Lead Bromide Perovskite Nanocrystals. Langmuir, 2020, 36, 13663-13669.	3.5	14
17	<p>Magnetic Targeting of HU-MSCs in the Treatment of Glucocorticoid-Associated Osteonecrosis of the Femoral Head Through Akt/Bcl2/Bad/Caspase-3 Pathway</p> . International Journal of Nanomedicine, 2020, Volume 15, 3605-3620.	6.7	14
18	Homologous cancerous cell membrane modulated multifunctional nanoshuttles: Targeting specificity and improved tumor theranostics. Composites Communications, 2020, 20, 100342.	6.3	13

#	Article	IF	CITATIONS
19	Ultrathin BiVO4 nanosheets sensing electrode for isopropanol sensor based on pyrochlore-Gd2Zr2O7 solid state electrolyte. Sensors and Actuators B: Chemical, 2020, 321, 128478.	7.8	13
20	Ultrathin BiOX (X = Cl, Br, I) Nanosheets with Exposed {001} Facets for Photocatalysis. ACS Applied Nano Materials, 2020, 3, 1981-1991.	5.0	100
21	Energy Level Modification with Carbon Dot Interlayers Enables Efficient Perovskite Solar Cells and Quantum Dot Based Lightâ€Emitting Diodes. Advanced Functional Materials, 2020, 30, 1910530.	14.9	72
22	Cesium–Lead Bromide Perovskite Nanoribbons with Two-Unit-Cell Thickness and Large Lateral Dimension for Deep-Blue Light Emission. ACS Applied Nano Materials, 2020, 3, 4826-4836.	5.0	8
23	Alginate mediated functional aggregation of gold nanoclusters for systemic photothermal therapy and efficient renal clearance. Carbohydrate Polymers, 2020, 241, 116344.	10.2	23
24	Schwann Cell Migration through Magnetic Actuation Mediated by Fluorescent–Magnetic Bifunctional Fe <sub>3</sub> O <sub>4</sub> ·Rhodamine 6G@Polydopamine Superparticles. ACS Chemical Neuroscience, 2020, 11, 1359-1370.	3.5	5
25	Advances in green colloidal synthesis of metal selenide and telluride quantum dots. Chinese Chemical Letters, 2019, 30, 277-284.	9.0	13
26	Tumor Microenvironment-Responsive Nanoshuttles with Sodium Citrate Modification for Hierarchical Targeting and Improved Tumor Theranostics. ACS Applied Materials & Interfaces, 2019, 11, 25730-25739.	8.0	29
27	Iron oxide nanoparticles promote the migration of mesenchymal stem cells to injury sites. International Journal of Nanomedicine, 2019, Volume 14, 573-589.	6.7	54
28	Multidrug resistant tumors-aimed theranostics on the basis of strong electrostatic attraction between resistant cells and nanomaterials. Biomaterials Science, 2019, 7, 4990-5001.	5.4	9
29	Paramagnetic CuS hollow nanoflowers for <i>T</i> <sub>2</sub> -FLAIR magnetic resonance imaging-guided thermochemotherapy of cancer. Biomaterials Science, 2019, 7, 409-418.	5.4	23
30	Targeting mitochondria with Au–Ag@Polydopamine nanoparticles for papillary thyroid cancer therapy. Biomaterials Science, 2019, 7, 1052-1063.	5.4	31
31	Oxygen-Defective Ultrathin BiVO <sub>4</sub> Nanosheets for Enhanced Gas Sensing. ACS Applied Materials & Interfaces, 2019, 11, 23495-23502.	8.0	81
32	<i>In vivo</i> migration of Fe <sub>3</sub> O <sub>4</sub> @polydopamine nanoparticle-labeled mesenchymal stem cells to burn injury sites and their therapeutic effects in a rat model. Biomaterials Science, 2019, 7, 2861-2872.	5.4	34
33	Aurophilic Interactions in the Selfâ€Assembly of Gold Nanoclusters into Nanoribbons with Enhanced Luminescence. Angewandte Chemie, 2019, 131, 8223-8228.	2.0	29
34	Aurophilic Interactions in the Selfâ€Assembly of Gold Nanoclusters into Nanoribbons with Enhanced Luminescence. Angewandte Chemie - International Edition, 2019, 58, 8139-8144.	13.8	185
35	Engineering the Photoluminescence of CsPbX <sub>3</sub> (X = Cl, Br, and I) Perovskite Nanocrystals Across the Full Visible Spectra with the Interval of 1 nm. ACS Applied Materials & Interfaces, 2019, 11, 14256-14265.	8.0	66
36	NF-κB inhibition promotes apoptosis in androgen-independent prostate cancer cells by the photothermal effect <i>via</i> the lκBα/AR signaling pathway. Biomaterials Science, 2019, 7, 2559-2570.	5.4	15

#	Article	IF	CITATIONS
37	Tumor Photothermal Therapy Employing Photothermal Inorganic Nanoparticles/Polymers Nanocomposites. Chinese Journal of Polymer Science (English Edition), 2019, 37, 115-128.	3.8	41
38	Polydopamine-coated Au-Ag nanoparticle-guided photothermal colorectal cancer therapy through multiple cell death pathways. Acta Biomaterialia, 2019, 83, 414-424.	8.3	68
39	Inorganic CsPbI <sub>2</sub> Br Perovskite Solar Cells: The Progress and Perspective. Solar Rrl, 2019, 3, 1800239.	5.8	217
40	Effect of Surface Trap States on Photocatalytic Activity of Semiconductor Quantum Dots. Journal of Physical Chemistry C, 2018, 122, 9312-9319.	3.1	22
41	Polymerâ€Passivated Inorganic Cesium Lead Mixedâ€Halide Perovskites for Stable and Efficient Solar Cells with High Openâ€Circuit Voltage over 1.3 V. Advanced Materials, 2018, 30, 1705393.	21.0	401
42	Post-healing of defects: an alternative way for passivation of carbon-based mesoscopic perovskite solar cells <i>via</i> hydrophobic ligand coordination. Journal of Materials Chemistry A, 2018, 6, 2449-2455.	10.3	66
43	Self-Assembly Driven Aggregation-Induced Emission of Copper Nanoclusters: A Novel Technology for Lighting. ACS Applied Materials & Interfaces, 2018, 10, 12071-12080.	8.0	93
44	Asymmetric surface modification of yeast cells for living self-assembly. Chemical Communications, 2018, 54, 14112-14115.	4.1	6
45	Cu–Fe–Se Ternary Nanosheet-Based Drug Delivery Carrier for Multimodal Imaging and Combined Chemo/Photothermal Therapy of Cancer. ACS Applied Materials & Interfaces, 2018, 10, 43396-43404.	8.0	52
46	Facile Synthesis of Cu–In–S/ZnS Core/Shell Quantum Dots in 1-Dodecanethiol for Efficient Light-Emitting Diodes with an External Quantum Efficiency of 7.8%. Chemistry of Materials, 2018, 30, 8939-8947.	6.7	70
47	Chloride treatment for highly efficient aqueous-processed CdTe nanocrystal-based hybrid solar cells. Journal of Materials Chemistry C, 2018, 6, 11156-11161.	5.5	2
48	Hollow Pd Nanospheres Conjugated with Ce6 To Simultaneously Realize Photodynamic and Photothermal Therapy. ACS Applied Bio Materials, 2018, 1, 1102-1108.	4.6	16
49	Microwave-Assisted Heating Method toward Multicolor Quantum Dot-Based Phosphors with Much Improved Luminescence. ACS Applied Materials & Interfaces, 2018, 10, 27160-27170.	8.0	21
50	Colloidal Synthesis of Ultrathin Monoclinic BiVO <sub>4</sub> Nanosheets for Z-Scheme Overall Water Splitting under Visible Light. ACS Catalysis, 2018, 8, 8649-8658.	11.2	151
51	Magnetic delivery of Fe <sub>3</sub> O <sub>4</sub> @polydopamine nanoparticle-loaded natural killer cells suggest a promising anticancer treatment. Biomaterials Science, 2018, 6, 2714-2725.	5.4	86
52	Photothermal-Activatable Fe <sub>3</sub> O <sub>4</sub> Superparticle Nanodrug Carriers with PD-L1 Immune Checkpoint Blockade for Anti-metastatic Cancer Immunotherapy. ACS Applied Materials & Interfaces, 2018, 10, 20342-20355.	8.0	112
53	Seedless preparation of Au nanorods by hydroquinone assistant and red blood cell membrane camouflage. RSC Advances, 2018, 8, 21316-21325.	3.6	18
54	Surfactant-Free Preparation of Au@Resveratrol Hollow Nanoparticles with Photothermal Performance and Antioxidant Activity. ACS Applied Materials & Interfaces, 2017, 9, 3376-3387.	8.0	35

#	Article	IF	CITATIONS
55	CsPb <sub><i>x</i></sub> Mn <sub>1–<i>x</i></sub> Cl <sub>3</sub> Perovskite Quantum Dots with High Mn Substitution Ratio. ACS Nano, 2017, 11, 2239-2247.	14.6	496
56	Constructing Postâ€Permeation Method to Fabricate Polymer/Nanocrystals Hybrid Solar Cells with PCE Exceeding 6%. Small, 2017, 13, 1603771.	10.0	16
57	Employing CdSe <sub><i>x</i></sub> Te <sub>1–<i>x</i></sub> Alloyed Quantum Dots to Avoid the Temperature-Dependent Emission Shift of Light-Emitting Diodes. Journal of Physical Chemistry C, 2017, 121, 5313-5323.	3.1	21
58	Phosphine-Free Synthesis of Metal Chalcogenide Quantum Dots by Directly Dissolving Chalcogen Dioxides in Alkylthiol as the Precursor. ACS Applied Materials & Interfaces, 2017, 9, 9840-9848.	8.0	20
59	Cu <sup>2+</sup> -Loaded Polydopamine Nanoparticles for Magnetic Resonance Imaging-Guided pH- and Near-Infrared-Light-Stimulated Thermochemotherapy. ACS Applied Materials & Interfaces, 2017, 9, 19706-19716.	8.0	103
60	Contribution of Metal Defects in the Assembly Induced Emission of Cu Nanoclusters. Journal of the American Chemical Society, 2017, 139, 4318-4321.	13.7	152
61	Aqueousâ€Processed Polymer/Nanocrystals Hybrid Solar Cells: The Effects of Chlorine on the Synthesis of CdTe Nanocrystals, Crystal Growth, Defect Passivation, Photocarrier Dynamics, and Device Performance. Solar Rrl, 2017, 1, 1600020.	5.8	24
62	Enzyme-Triggered Defined Protein Nanoarrays: Efficient Light-Harvesting Systems to Mimic Chloroplasts. ACS Nano, 2017, 11, 938-945.	14.6	71
63	Engineering a red emission of copper nanocluster self-assembly architectures by employing aromatic thiols as capping ligands. Nanoscale, 2017, 9, 12618-12627.	5.6	87
64	Seed-mediated phase-selective growth of Cu <sub>2</sub> GeS <sub>3</sub> hollow nanoparticles with huge cavities. CrystEngComm, 2017, 19, 6736-6743.	2.6	5
65	High-Efficiency Aqueous-Processed Polymer/CdTe Nanocrystals Planar Heterojunction Solar Cells with Optimized Band Alignment and Reduced Interfacial Charge Recombination. ACS Applied Materials & Interfaces, 2017, 9, 31345-31351.	8.0	29
66	Engineering the Self-Assembly Induced Emission of Cu Nanoclusters by Au(I) Doping. ACS Applied Materials & Interfaces, 2017, 9, 24899-24907.	8.0	69
67	Cu(II)-Doped Polydopamine-Coated Gold Nanorods for Tumor Theranostics. ACS Applied Materials & Interfaces, 2017, 9, 44293-44306.	8.0	45
68	One-Step Preparation of Cesium Lead Halide CsPbX <sub>3</sub> (X = Cl, Br, and I) Perovskite Nanocrystals by Microwave Irradiation. ACS Applied Materials & Interfaces, 2017, 9, 42919-42927.	8.0	117
69	Analogous self-assembly and crystallization: a chloride-directed orientated self-assembly of Cu nanoclusters and subsequent growth of Cu <sub>2â^'x</sub> S nanocrystals. Nanoscale, 2017, 9, 10335-10343.	5.6	6
70	Electrostatic attraction driven and shuttle-like morphology assisted enhancement for tumor uptake. RSC Advances, 2017, 7, 56621-56628.	3.6	4
71	Copper inter-nanoclusters distance-modulated chromism of self-assembly induced emission. Nanoscale, 2017, 9, 18845-18854.	5.6	29
72	Facile Synthesis of Cu <sub>2</sub> GeS <sub>3</sub> and Cu <sub>2</sub> MGeS <sub>4</sub> (M = Zn,) Tj E	ΓQq0 0 0 ι 6.7	gBT /Overloci 22

#	Article	IF	CITATIONS
73	Cu(II) doped polyaniline nanoshuttles for multimodal tumor diagnosis and therapy. Biomaterials, 2016, 104, 213-222.	11.4	48
74	Fe <sub>3</sub> O <sub>4</sub> @polydopamine Composite Theranostic Superparticles Employing Preassembled Fe <sub>3</sub> O <sub>4</sub> Nanoparticles as the Core. ACS Applied Materials & Interfaces, 2016, 8, 22942-22952.	8.0	135
75	Solution-Processed, Ultrathin Solar Cells from CdCl <sub>3</sub> <sup>–</sup> -Capped CdTe Nanocrystals: The Multiple Roles of CdCl <sub>3</sub> <sup>–</sup> Ligands. Journal of the American Chemical Society, 2016, 138, 7464-7467.	13.7	64
76	Aqueous-Processed Insulating Polymer/Nanocrystal Hybrid Solar Cells. ACS Applied Materials & Interfaces, 2016, 8, 7101-7110.	8.0	23
77	Seedless synthesis of gold nanorods using resveratrol as a reductant. Nanotechnology, 2016, 27, 165601.	2.6	21
78	Electrophoretic deposition of fluorescent Cu and Au sheets for light-emitting diodes. Nanoscale, 2016, 8, 395-402.	5.6	21
79	Hydroquinone-Assisted Synthesis of Branched Au–Ag Nanoparticles with Polydopamine Coating as Highly Efficient Photothermal Agents. ACS Applied Materials & Interfaces, 2015, 7, 11613-11623.	8.0	95
80	Self-Assembly of Nanoclusters into Mono-, Few-, and Multilayered Sheets <i>via</i> Dipole-Induced Asymmetric van der Waals Attraction. ACS Nano, 2015, 9, 6315-6323.	14.6	98
81	Surface Ligand Dynamics-Guided Preparation of Quantum Dots–Cellulose Composites for Light-Emitting Diodes. ACS Applied Materials & Interfaces, 2015, 7, 15830-15839.	8.0	57
82	Efficient aqueous-processed hybrid solar cells from a polymer with a wide bandgap. Journal of Materials Chemistry A, 2015, 3, 10969-10975.	10.3	30
83	Assembly-Induced Enhancement of Cu Nanoclusters Luminescence with Mechanochromic Property. Journal of the American Chemical Society, 2015, 137, 12906-12913.	13.7	367
84	Phosphine-free synthesis of Ag–In–Se alloy nanocrystals with visible emissions. Nanoscale, 2015, 7, 18570-18578.	5.6	32
85	Aqueous-Processed Inorganic Thin-Film Solar Cells Based on CdSe <sub><i>x</i></sub> Te <sub>1–<i>x</i></sub> Nanocrystals: The Impact of Composition on Photovoltaic Performance. ACS Applied Materials & Interfaces, 2015, 7, 23223-23230.	8.0	48
86	Cupreous Complex-Loaded Chitosan Nanoparticles for Photothermal Therapy and Chemotherapy of Oral Epithelial Carcinoma. ACS Applied Materials & Interfaces, 2015, 7, 20801-20812.	8.0	58
87	Hydrazine-Mediated Construction of Nanocrystal Self-Assembly Materials. ACS Nano, 2014, 8, 10569-10581.	14.6	40
88	Deriving the colloidal synthesis of crystalline nanosheets to create self-assembly monolayers of nanoclusters. Advances in Colloid and Interface Science, 2014, 207, 347-360.	14.7	16
89	In Situ Construction of Nanoscale CdTe dS Bulk Heterojunctions for Inorganic Nanocrystal Solar Cells. Advanced Energy Materials, 2014, 4, 1400235.	19.5	44
90	Polypyrrole-Coated Chainlike Gold Nanoparticle Architectures with the 808 nm Photothermal Transduction Efficiency up to 70%. ACS Applied Materials & Interfaces, 2014, 6, 5860-5868.	8.0	83

#	Article	IF	CITATIONS
91	Quantum-Dot-Induced Self-Assembly of Cricoid Protein for Light Harvesting. ACS Nano, 2014, 8, 3743-3751.	14.6	83
92	Composite Photothermal Platform of Polypyrrole-Enveloped Fe <sub>3</sub> O <sub>4</sub> Nanoparticle Self-Assembled Superstructures. ACS Applied Materials & Interfaces, 2014, 6, 14552-14561.	8.0	108
93	Colloidal Selfâ€Assembly of Catalytic Copper Nanoclusters into Ultrathin Ribbons. Angewandte Chemie - International Edition, 2014, 53, 12196-12200.	13.8	78
94	Synthesis of a Waterâ€Soluble Conjugated Polymer Based on Thiophene for an Aqueousâ€Processed Hybrid Photovoltaic and Photodetector Device. Advanced Materials, 2014, 26, 3655-3661.	21.0	35
95	A totally phosphine-free synthesis of metal telluride nanocrystals by employing alkylamides to replace alkylphosphines for preparing highly reactive tellurium precursors. Nanoscale, 2013, 5, 9593.	5.6	12
96	Alkylthiol-Enabled Se Powder Dissolution in Oleylamine at Room Temperature for the Phosphine-Free Synthesis of Copper-Based Quaternary Selenide Nanocrystals. Journal of the American Chemical Society, 2012, 134, 7207-7210.	13.7	213
97	Controllable Synthesis of Stable Urchin-like Gold Nanoparticles Using Hydroquinone to Tune the Reactivity of Gold Chloride. Journal of Physical Chemistry C, 2011, 115, 3630-3637.	3.1	196
98	Simple Synthesis of Highly Luminescent Water-Soluble CdTe Quantum Dots with Controllable Surface Functionality. Chemistry of Materials, 2011, 23, 4857-4862.	6.7	124
99	Growth Kinetics of Aqueous CdTe Nanocrystals in the Presence of Simple Amines. Journal of Physical Chemistry C, 2010, 114, 6418-6425.	3.1	37
100	Nucleation of Aqueous Semiconductor Nanocrystals: A Neglected Factor for Determining the Photoluminescence. Journal of Physical Chemistry C, 2010, 114, 22487-22492.	3.1	24
101	"One-pot―synthesis and shape control of ZnSe semiconductor nanocrystals in liquid paraffin. Journal of Materials Chemistry, 2010, 20, 4451.	6.7	26
102	Manipulating the growth of aqueous semiconductor nanocrystals through amine-promoted kinetic process. Physical Chemistry Chemical Physics, 2010, 12, 332-336.	2.8	21
103	The Influence of Carboxyl Groups on the Photoluminescence of Mercaptocarboxylic Acid-Stabilized CdTe Nanoparticles. Journal of Physical Chemistry B, 2003, 107, 8-13.	2.6	581